JOURNAL OF CATALYSIS **168,** 491–500 (1997)
ARTICLE NO. CA971650

Kinetics of the Hydrodenitrogenation of *ortho*-Propylaniline over $NiMo(P)/Al_2O_3$ Catalysts

M. Jian, F. Kapteijn,[1] and R. Prins

Laboratory for Technical Chemistry, Federal Institute of Technology (ETH), 8092 Zürich, Switzerland

Received November 19, 1996; revised February 4, 1997; accepted February 5, 1997

The kinetics of the hydrodenitrogenation (HDN) of *ortho*-propylaniline (OPA) was studied over sulfided $NiMo(P)/Al_2O_3$ catalysts. A small amount of propylcyclohexylamine was observed in the reaction product, demonstrating that hydrogenation of the phenyl group of OPA was one of the first and rate-limiting steps in the HDN reaction. A Langmuir–Hinshelwood kinetic model with different sites for the HDN and hydrogenation could successfully fit the reaction network. Some kinetic parameters were obtained by varying the initial reactant partial pressure at constant space time and by simultaneous reaction, while others were determined by varying the space time at constant reactant partial pressure. The HDN rate constants and the adsorption constants of OPA and NH_3 were higher over the phosphate-containing catalyst than over the phosphate-free catalyst, while the activation energies as well as the heats of adsorption of OPA did not show any difference between the two catalysts. This demonstrates that the nature of the catalyst sites did not change by the introduction of phosphate. The promotive effect of phosphorus in the HDN of OPA arises from an increased number of active sites for the hydrogenation of the phenyl ring of OPA as well as from a stronger adsorption of OPA due to increased MoS_2 stacking and therefore less hindered adsorption. Phosphorus shows a promotive effect on the hydrogenation of pure olefins, but a negative effect when nitrogen-containing compounds are present. This is due to a stronger adsorption of the nitrogen-containing compounds on the P-containing catalyst, and hence to a stronger inhibition.

INTRODUCTION

Anilines represent an important class of nitrogen-containing hydrocarbons in petroleum distillates. Although the hydrodenitrogenation (HDN) of pure anilines is relatively easy, this denitrogenation reaction is almost completely inhibited when other basic nitrogen-containing compounds are present in the feedstock, as always is the case in industrial HDN processes (1–4). This influence of basic nitrogen-containing compounds has been interpreted by competitive adsorption caused by differences in basicity or proton affinity of these compounds toward the catalyst (5–8). It has been reported that the adsorption constants of quinoline-type compounds are 5–20 times larger than those of alkylanilines (6). Therefore, anilines will have very little chance to adsorb and thus to react on the catalyst surface when quinoline-type compounds are still present. In a study of the hydrotreatment of coked gasoil on $NiMo/Al_2O_3$ catalysts, Kasztelan *et al.* (9) reported that before hydrotreatment almost no alkylanilines were present in the feed, whereas the concentration of these molecules was substantial in the effluent, suggesting that in the HDN of real feedstocks heterocyclic nitrogen-containing compounds can be relatively easily converted to aniline-type compounds, but that the further conversion of these anilines may be difficult. Therefore, a high denitrogenation conversion can only be obtained if these anilines are converted. Nevertheless, only few HDN studies of anilines have been conducted (10–14).

It has been reported that the promotive effect of phosphorus over $NiMo(P)/Al_2O_3$ catalysts on the HDN reaction of quinoline arises partly from its accelerating ability on the conversion of the alkylaniline intermediate (15). However, whether this positive effect of phosphorus comes from the intrinsic promotive effect of phosphorus in the HDN reaction of quinoline through the *ortho*-propylaniline (OPA) reaction pathway, or whether it is due to a different adsorption strength of nitrogen-containing compounds on the HDN catalytic sites over phosphorus-containing $NiMo/Al_2O_3$ catalysts, needs further investigation. A study of these phenomena will certainly be helpful in understanding the functioning of the HDN catalyst and the reaction mechanism, and will lead to the improvement of the industrial process.

In the present work, OPA is employed as the model reaction compound. OPA is formed as a key intermediate in the HDN of quinoline, and is one of the representative alkylanilines in oil distillates. The study of the HDN mechanism and kinetics of OPA was carried out over $NiMo(P)/Al_2O_3$ catalysts at 593–643 K and 3.0 MPa, with emphasis on the role of phosphorus. Hydrogenation of cyclohexene and ethylbenzene was also performed under HDN conditions in order to elucidate the elementary reaction steps.

[1] Permanent address: Faculty of Chemical Technology and Materials Science, Delft University of Technology, 2628 BL Delft, The Netherlands.

0021-9517/97 $25.00

TABLE 1

Typical Reaction Stream Composition

Reactant	Partial pressure (kPa)	Reference
Hydrogen	2890	Reactant
Octane	92.2–98.1	Solvent
Hydrogen sulfide	6.5	H_2S
n-Nonane	2.1	Internal standard
n-Dodecane	2.1	Internal standard
ortho-Propylaniline	1.2–7.1	Reactant

EXPERIMENTAL

Catalysts used in this work had a composition of 3 wt% nickel, 8 wt% molybdenum, and 0 or 2 wt% phosphorus. Details of the catalyst preparation can be found elsewhere (16). The HDN reactions were carried out in a continuous-flow microreactor. A sample of 0.1 g catalyst diluted with 9.5 g SiC was sulfided *in situ* with a mixture of 10% (mol) H_2S and H_2 at 643 K and 1.5 MPa for 4 h. After sulfidation the pressure was increased to 3.0 MPa and liquid reactant was fed to the reactor by means of a high-pressure pump, with *n*-octane as the solvent. Dimethyldisulfide (DMDS) was added to the liquid reactant to generate H_2S in the reaction stream ($P_{H_2S} = 6.5$ kPa). The gas-phase reactant composition is given in Table 1.

Reaction products were analyzed by on-line gas chromatography with a Shimadzu GC-14A gas chromatograph equipped with a 30-m DB-5 fused silica capillary column (J&W, 0.32-mm i.d., 0.25-μm film thickness) and a flame ionization detector. Samples were taken after 100 h on stream at 643 K when the activity of the catalyst was relatively stable, with *n*-nonane and *n*-dodecane as internal standards. Space time was defined as $\tau = \varepsilon \cdot V_{cat}/\nu_{gas}$, where ε is the void fraction of the catalyst bed (assumed to be equal to 0.4), V_{cat} is the volume of the catalyst, and ν_{gas} is the total volume flow rate of the gas-phase reactant. The space time (τ) was changed by varying the liquid and gaseous reactant flow rates while keeping their ratios constant.

The inhibitory effect of NH_3 on the hydrogenation of cyclohexene (CHE), which resembles the reaction intermediate propylcyclohexene (PCHE), was studied by adding pentylamine to the feed to generate NH_3 in the reaction stream.

RESULTS

1. HDN Reaction Scheme of OPA

The HDN reaction network of OPA is shown in Fig. 1a. There are two reaction pathways in the HDN of OPA over sulfided NiMo(P)/Al_2O_3 catalysts: direct C(sp^2)–N bond cleavage under the formation of propylbenzene (PB) (path 1), and hydrogenation of the aromatic ring to propylcyclohexylamine (PCHA), followed by an elimination of NH_3 to PCHE, with subsequent reaction to PB or propylcyclohexane (PCH) (path 2) (11, 13). The result of the hydrogenation of ethylbenzene (EB) in the presence of OPA showed that even at the largest space time of our HDN reaction conditions, hydrogenation of aromatics hardly occurred (Table 2). Therefore, the PB → PCH reaction was neglected in our kinetic analysis of the HDN of OPA.

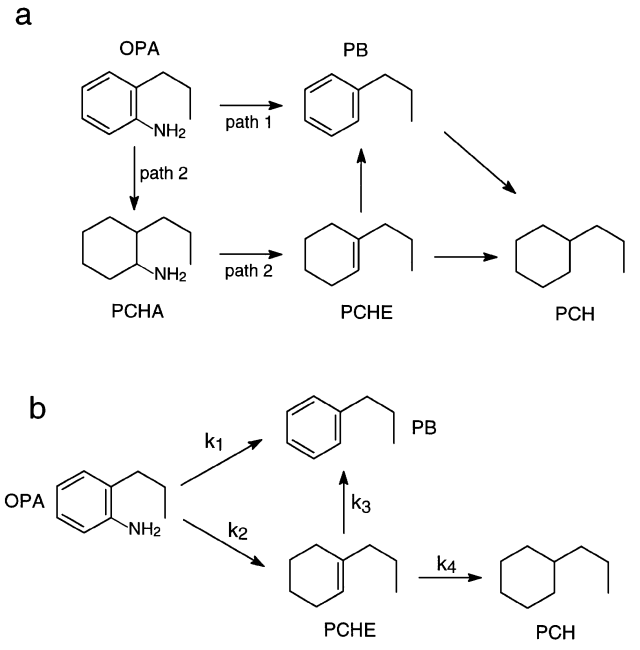

FIG. 1. (a) HDN reaction network of *ortho*-propylaniline. (b) Simplified kinetic network of the HDN of *ortho*-propylaniline.

Small amounts of PCHA were observed in the HDN product of OPA at short space time (Table 3), demonstrating that a first reaction step in the HDN of OPA is saturation of the phenyl group, to form the same PCHA intermediate as in the HDN of quinoline (Q) and decahydroquinoline (DHQ) (17, 18). PCHA was observed only in the absence of H_2S in the HDN of OPA, while in the HDN of DHQ and Q it was mainly observed in the presence of H_2S (19). This indicates that the rate-limiting reaction steps in the conversions of DHQ and OPA are different. It is well known that H_2S promotes elimination reactions and inhibits hydrogenation

TABLE 2

Hydrogenation of Ethylbenzene (EB) in the Presence of OPA at 3.0 MPa and $\tau = 0.51$ s ($P^0_{OPA} = 4.8$ kPa, $P^0_{EB} = 1.6$ kPa, $P_{H_2S} = 6.5$ kPa)

	EB conversion (%)		
Catalyst	593 K	623 K	643 K
NiMo/Al_2O_3	0.5	1.0	2.5
NiMoP(2)/Al_2O_3	0.2	0.7	1.9

TABLE 3

Products of the HDN of OPA and DHQ at 593 K, 3.0 MPa, and $\tau = 0.11$ s over NiMoP/Al_2O_3

Reactant	H_2S (kPa)	Composition (%)					
		PCH	PCHE	PB	PCHA	OPA	DHQ
OPA	6.5	1.9	4.9	0.4	0	92.7	0
OPA	0	5.3	4.9	2.1	0.2	86.1	0
DHQ	6.5	0.6	0.9	0	1.5	/	97.0[a]
DHQ	0	0.4	0.7	0.1	0.1	/	98.7[a]

[a] Including a small amount of 5,6,7,8-tetrahydroquinoline and 1,2,3,4-tetrahydroquinoline.

reactions over NiMo/Al_2O_3 catalyst (20–26). The observation of PCHA in the absence, but not in the presence, of H_2S suggests that the hydrogenation of OPA to PCHA is a relatively slow reaction step in the HDN of OPA, especially in the presence of H_2S. Only when this reaction step is accelerated and the subsequent reaction step slowed down, as in the absence of H_2S, can the intermediate PCHA be observed. In contrast, H_2S exhibits a stronger accelerating effect on the first C–N bond cleavage of DHQ → PCHA in the HDN of DHQ.

Since the concentration of PCHA was always quite low in the HDN product of OPA, kinetically PCHE can be considered a primary HDN product, as demonstrated by the HDN product composition versus space time plot (Fig. 2). Therefore, the intermediate PCHA was omitted from the kinetic analysis, and the kinetic analysis was performed on the scheme presented in Fig. 1b.

2. *Kinetic Modeling*

It has been suggested that direct C(sp^2)–X (X = S, O, N) bond cleavage takes place on a different catalytic site than hydrogenation reactions in the catalytic hydrodesulfurization (HDS), hydrodeoxygenation (HDO), and HDN over sulfided NiMo(P)/Al_2O_3 catalysts (13, 27–32). However, under the present reaction conditions the extent of direct C(sp^2)–N bond cleavage in the HDN of OPA was usually below 10% of the overall HDN conversion (see below, Table 5). Therefore, and because of the experimental uncertainties, no distinction was made between these catalytic sites in the kinetic modeling. To simplify the kinetic calculations, it was assumed that OPA exhibits the same adsorption constant on the catalytic sites used in reaction path 1 and path 2 (Fig. 1).

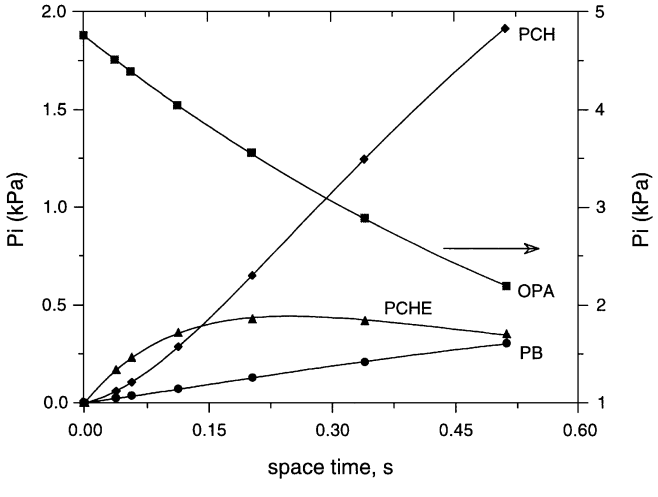

FIG. 2. Product composition versus space time in the HDN of OPA over NiMoP/Al_2O_3 at 623 K and 3.0 MPa.

Hydrogenation of olefins, however, has been demonstrated to take place on a different catalytic site than the ring opening and N-removal elimination reactions of piperidine and decahydroquinoline (18). In Section 2.2 we will show that the same holds for the hydrogenation of cyclohexene (CHE) and the HDN of OPA. Furthermore, if the HDN of OPA and hydrogenation of CHE could occur on the same catalytic site and follow a Langmuir–Hinshelwood mechanism, we would have for a simultaneous reaction of OPA and CHE

$$\ln(1 - x_{\mathrm{OPA}}) = \frac{(k_1 + k_2)K_{\mathrm{OPA}}}{k_{\mathrm{CHE}}K_{\mathrm{CHE}}} \cdot \ln(1 - x_{\mathrm{CHE}}), \qquad [1]$$

where x_{OPA} and x_{CHE} are respectively the conversions of OPA and CHE, k_1 and k_2 are respectively the HDN rate constants via reaction paths 1 and 2, k_{CHE} is the rate constant of the hydrogenation of CHE, K_{CHE} is the adsorption constant of CHE, and K_{OPA} is the adsorption constant of OPA on the catalytic site for the HDN reaction. A plot of $\ln(1 - x_{\mathrm{OPA}})$ versus $\ln(1 - x_{\mathrm{CHE}})$ should give a straight line if the two reactions would take place over the same catalytic site. The curvature in Fig. 3 is in agreement with the presence of different catalytic sites in the hydrogenation of CHE and the HDN of OPA.

Direct simulation of all the experimental results of the HDN of OPA with the Langmuir–Hinshelwood kinetic model did not give unique parameter values. When one of the parameters was varied by a factor of 10, the other parameters could adapt reasonably well and the resulting fit was still acceptable. Therefore, other methods for determining the kinetic parameters had to be found.

2.1. Influence of the initial reactant partial pressure (P^0_{OPA}). Assuming that a Langmuir–Hinshelwood description applies for the reaction network of Fig. 1b, and that the adsorption of the nitrogen-free hydrocarbons (PCH, PCHE, PB, and the solvent) in the reaction stream can be neglected, the HDN reaction rate of OPA can be written as

$$-\frac{dP_{\mathrm{OPA}}}{d\tau} = \frac{(k_1 + k_2)K_{\mathrm{OPA}}P_{\mathrm{OPA}}}{1 + K_{\mathrm{OPA}}P_{\mathrm{OPA}} + K_{\mathrm{NH_3}}P_{\mathrm{NH_3}}} \qquad [2]$$

$$P_{\mathrm{NH_3}} = P^0_{\mathrm{OPA}} - P_{\mathrm{OPA}} \qquad [3]$$

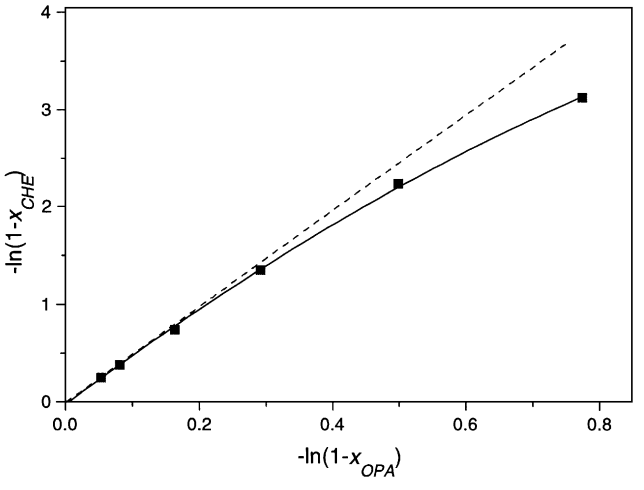

FIG. 3. Simultaneous hydrogenation of CHE and HDN of OPA at 623 K and 3.0 MPa over NiMoP/Al_2O_3.

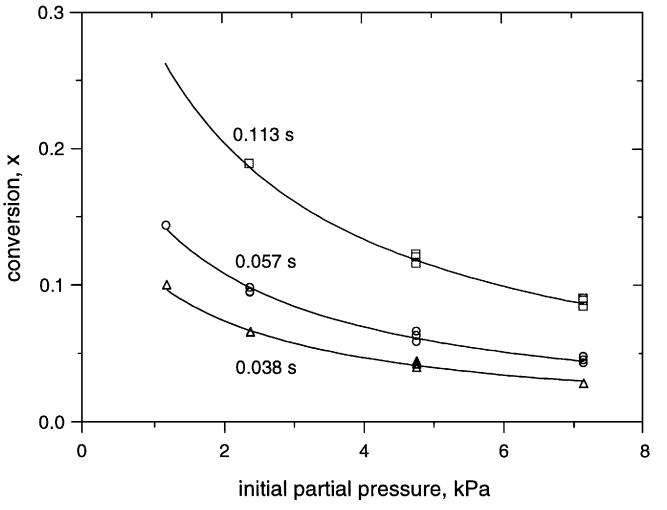

FIG. 4. Dependence of the HDN conversion of OPA as a function of the initial partial pressure at different space times over NiMo/Al_2O_3 at 623 K and 3.0 MPa (points, experimental data; lines, prediction).

$$1 + K_{\mathrm{OPA}} P_{\mathrm{OPA}} + K_{\mathrm{NH_3}} P_{\mathrm{NH_3}} = 1 + K_{\mathrm{OPA}} P^0_{\mathrm{OPA}} + (K_{\mathrm{NH_3}} - K_{\mathrm{OPA}})\left(P^0_{\mathrm{OPA}} - P_{\mathrm{OPA}}\right), \quad [4]$$

where τ is the space time, P_{OPA} and $P_{\mathrm{NH_3}}$ are respectively the partial pressures of OPA and NH_3 in the reaction stream (P^0_{OPA} is the initial partial pressure of OPA), k_1 and k_2 are respectively the HDN reaction rate constants through reaction paths 1 and 2 (Fig. 1), and K_{OPA} and $K_{\mathrm{NH_3}}$ are the Langmuir adsorption constants of OPA and NH_3 on the catalytic sites for the HDN reaction, respectively.

If the reaction is performed at low conversion (<20%), the last term in Eq. [4] can be neglected and we get

$$-\ln(1 - x_{\mathrm{OPA}}) = \frac{(k_1 + k_2)K_{\mathrm{OPA}}}{1 + K_{\mathrm{OPA}} P^0_{\mathrm{OPA}}} \cdot \tau, \quad [5]$$

where x_{OPA} is the conversion of OPA. At a fixed space time, a series of x_{OPA} values is obtained by varying the initial partial pressure of OPA. Thus, the sum of the rate constants $k_1 + k_2$ and the adsorption constant K_{OPA} can be determined through nonlinear regression of Eq. [5], minimizing the sum of the squared residuals of the conversion values. An example of such a regression is given in Fig. 4.

The individual values of k_1 and k_2 can be obtained in combination with the initial slope of the $1 - x_{\mathrm{OPA}}$ versus x_{PB} (conversion to PB) plot which gives the ratio of k_2/k_1 (13, 28), once the sum of $k_1 + k_2$ is obtained. Figure 5 gives an example.

$$1 - x_{\mathrm{OPA}} = \frac{k_1 + k_2}{k_1} \cdot x_{\mathrm{PB}}. \quad [6]$$

2.2. The inhibition adsorption of NH_3 and OPA. The final HDN product NH_3 also adsorbs strongly on the catalytic sites and inhibits the HDN and hydrogenation reactions (3). In practice, the inhibition adsorption constants of NH_3 can only be properly determined at high HDN conversions when the relative concentration of NH_3 in the reaction stream is high, since only under this condition will the inhibition effect of NH_3 have a significant influence on the HDN reaction. To simulate such a situation, ammonia precursors (pentylamine, diaminopropane, and ammonium carbonate) have been introduced to the reactant to generate a certain concentration of NH_3 *in situ* (6, 25, 28).

It was found that when pentylamine (1.6 kPa) was added to the HDN reactant of OPA, the mass balance of pentylamine was poor at low OPA conversions. A similar situation has been reported by La Vopa and Satterfield (6) when saturated amines were added to the HDS reaction of thiophene. Although the mass balance was improved at high

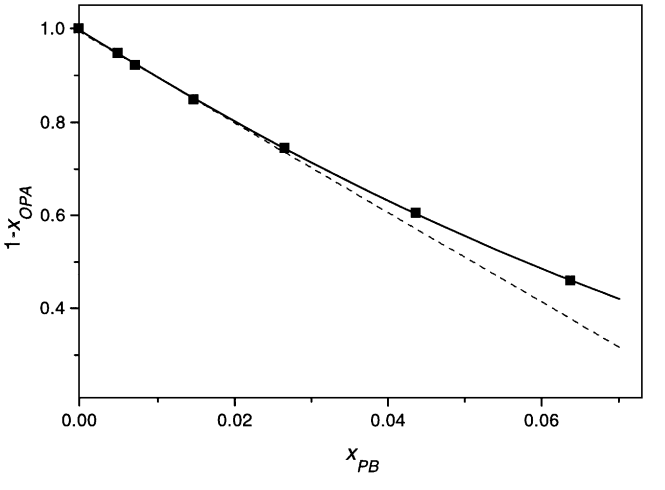

FIG. 5. Determination of k_2/k_1 in the HDN network of OPA over NiMoP/Al_2O_3 at 623 K, 3.0 MPa, and $P^0_{\mathrm{OPA}} = 4.8$ kPa.

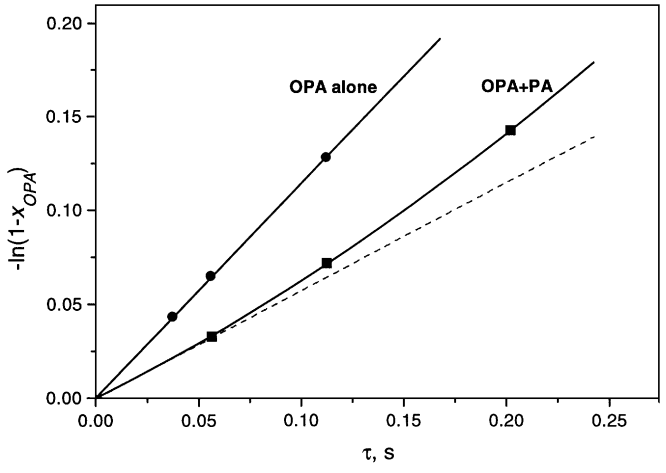

FIG. 6. Inhibition effect of pentylamine (PA) on the HDN of OPA at 593 K and 3.0 MPa over NiMo/Al_2O_3 ($P^0_{OPA} = 4.8$ kPa, $P^0_{PA} = 1.6$ kPa).

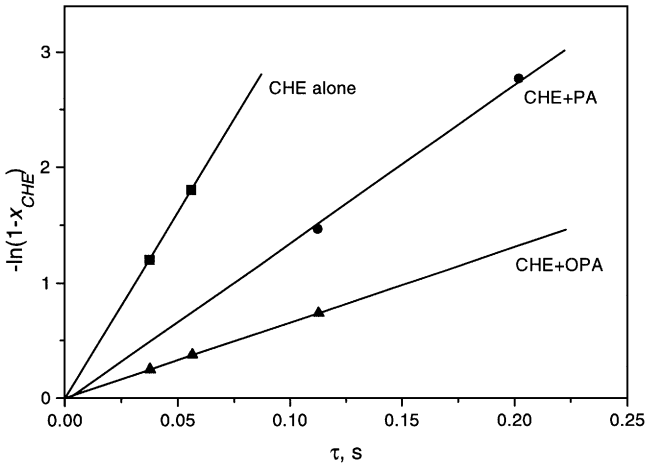

FIG. 7. Hydrogenation of CHE over NiMoP/Al_2O_3 at 623 K and 3.0 MPa ($P^0_{CHE} = 1.6$ kPa, $P^0_{OPA} = 4.8$ kPa, $P^0_{PA} = 1.6$ kPa).

reaction temperatures and conversions, the data cannot be simply handled to calculate K_{NH_3} since under these conditions one cannot neglect the formation of NH_3 from the HDN reaction itself and assume that $P_{OPA} = P^0_{OPA}$ in the denominator of Eq. [2]. The $-\ln(1 - x_{OPA})$ versus τ plot in the presence of pentylamine curves upward (Fig. 6), indicating that the adsorption of pentylamine (or of imine or nitrile intermediates) was stronger than that of NH_3. For these reasons, we preferred to determine the adsorption constant of NH_3 (K_{NH_3}) on the HDN site through fitting of the HDN network.

Since hydrogenation of the olefin takes place on a different catalytic site than the HDN of OPA, the inhibition adsorption constants of OPA and NH_3 on these catalytic sites should be different. In the present case, the olefin hydrogenation reaction step in the HDN of OPA (PCHE → PCH) was studied by using CHE as the model reactant under the HDN reaction conditions, as PCHE was not commercially available. The inhibition adsorption constant of a nitrogen-containing compound i ($i = NH_3$ or OPA) on this hydrogenation reaction was calculated with the aid of Eq. [7],

$$-\ln(1 - x_{CHE}) = \frac{k_{CHE} K_{CHE}}{1 + K'_i P_i} \cdot \tau, \qquad [7]$$

where K'_i is the adsorption constant of the inhibitor on the hydrogenation site, and P_i is the partial pressure of the inhibitor in the reaction stream. The adsorption constant of NH_3 on the catalytic site of the hydrogenation reaction was determined through hydrogenation of CHE in the presence of pentylamine, since in this case it was not necessary to assume that $P_{CHE} = P^0_{CHE}$ as the adsorption of CHE was weak and could be neglected. The reaction was carried out at high conversions to get a good mass balance of pentylamine. The adsorption constant of OPA on the hydrogenation site was determined by simultaneous reaction of OPA + CHE, and the reaction was performed at low OPA conversions so that a constant P^0_{OPA} in the denominator of Eq. [7] could be assumed.

Since $k_{CHE}K_{CHE}$ can be obtained from the hydrogenation of CHE in the absence of i ($P_i = 0$, first-order reaction), K'_i is calculated from the slope of the $-\ln(1 - x_{CHE})$ versus τ plot in the presence of compound P_i, as shown in Fig. 7.

3. *Kinetic Parameters*

3.1. HDN reaction rate and adsorption constants. From the regression of the HDN results of different OPA initial partial pressures at low conversions, the HDN rate constant ($k_1 + k_2$) and the adsorption constant of OPA (K_{OPA}) on the HDN site were determined. Table 4 gives the values of these constants over the NiMo/Al_2O_3 and NiMoP/Al_2O_3 catalysts at 593–643 K and 3.0 MPa. The 95% confidence range of the rate constants was usually within ±10% of the parameter values, while the 95% confidence range of

TABLE 4

Rate and Adsorption Constants from the Regression of the HDN Results at Different OPA Initial Partial Pressures at Low Conversions

Catalyst	Temp. (K)	$k_1 + k_2$ (kPa · s^{-1})	Confidence[a] Low	Confidence[a] High	K_{OPA} (kPa^{-1})	Confidence[a] Low	Confidence[a] High
NiMo	593	2.0	1.9	2.1	1.4	1.2	1.7
NiMoP	593	2.3	2.2	2.4	2.4	1.9	2.9
NiMo	623	6.8	6.5	7.1	0.75	0.66	0.84
NiMoP	623	8.0	7.7	8.2	1.2	1.0	1.4
NiMo	643	14.5	13.7	15.2	0.46	0.39	0.52
NiMoP	643	15.6	14.8	16.3	0.82	0.70	0.93

[a] 95% confidence range.

TABLE 5

Rate Constants in the HDN Network of OPA over NiMo(P)/Al_2O_3 at 593–643 K, 3.0 MPa, and $P_{H_2S} = 6.5$ kPa [kPa · s^{-1}]

Catalyst	Temp. (K)	$(k_1+k_2)/k_1$	k_1	k_2	Effective[a]
NiMo/Al_2O_3	593	21	0.10	1.9	0.37
NiMoP2/Al_2O_3	593	14	0.16	2.1	0.44
NiMo/Al_2O_3	623	15	0.45	6.3	1.1
NiMoP2/Al_2O_3	623	9.7	0.82	7.2	1.4
NiMo/Al_2O_3	643	9.5	1.6	13	2.1
NiMoP2/Al_2O_3	643	6.5	2.4	13.4	2.6

[a] Effective rate constant ($((k_1+k_2)K_{OPA}/(1+K_{OPA}P^0_{OPA})$) at $P^0_{OPA} =$ 4.8 kPa.

the adsorption constants was usually within ±20% of the parameter values. These results indicate that the regression method was relevant for the experimental data.

The adsorption constants of OPA (K_{OPA}) obtained for the HDN of OPA itself (Table 4) are much larger than those obtained from the inhibition effect of aniline or on the HDS of thiophene at 623 K and 7.0 MPa over a commercial NiMo/Al_2O_3 catalyst (6). Besides the differences in the catalysts and the reaction conditions, we believe that the differences in the nature of the catalytic sites for these different reactions account for the difference in the adsorption constants. Therefore, special attention must be paid in determining adsorption constants through the inhibition effect; they may be valid only for the reaction under study. This is further demonstrated by the CHE hydrogenation results in Section 3.2.

The individual rate constants k_1 and k_2 are given in Table 5. Tables 4 and 5 show that introduction of phosphorus to a NiMo/Al_2O_3 catalyst increases the reaction rate constants of both HDN paths, but to a greater extent that of path 1 (Fig. 1), as well as the adsorption constants of OPA. The resulting effective rate constants for OPA conversion $(k_1+k_2)K_{OPA}/(1+K_{OPA}P^0_{OPA})$ are higher over the P-containing catalyst which accounts for the overall promotive effect of phosphorus over the NiMoP/Al_2O_3 catalyst.

The higher values of the rate constants show that the number and/or the intrinsic activity of the catalytic sites for the HDN of OPA were higher over the NiMoP/Al_2O_3 catalyst than over the NiMo/Al_2O_3 catalyst. The higher adsorption constants indicate that the properties of the HDN sites were modified by the presence of phosphorus. Since phosphorus decreases the specific surface area and pore volume of the oxidic NiMo/Al_2O_3 catalyst (33), it is logical to assume that the catalytic sites for the HDN of OPA are due to a special geometry or electric feature of the active phase which is different from that for the HDN of piperidine and decahydroquinoline, where the activity decreases as the specific surface area and pore volume of the catalyst decrease (15).

3.2. The inhibition adsorption constant on the hydrogenation site. In the simultaneous reaction of CHE and OPA, it was found that the presence of CHE had no influence on the HDN conversion of OPA, showing that the adsorption of CHE is weak and can be neglected in the rate equations of the HDN reactions. This also confirms the validity of the assumption in Eqs. [2]–[7] that the adsorption of the nitrogen-free hydrocarbons can be neglected. However, the presence of OPA and NH_3 in the reaction stream strongly inhibited the hydrogenation reaction of CHE, as shown in Fig. 7. The effective rate constants of CHE hydrogenation and adsorption constants of OPA and NH_3 on the catalytic site of CHE hydrogenation reaction are given in Table 6.

A comparison of Tables 4 and 6 clearly demonstrates that OPA has different adsorption constants on the catalytic sites of the HDN of OPA and the hydrogenation of CHE. The inhibition adsorption constants for the former case were higher than those for the latter case, especially at low reaction temperatures, even though the slow reaction step in both cases is a hydrogenation reaction. In the first case a phenyl group associated with an amine group is involved and in the second case an alkene group is involved. This observation indicates that the catalytic site for the hydrogenation of a phenyl group in an aniline molecule is different from that of an olefinic group. In addition, the inhibition adsorption constants of OPA and NH_3 on the catalytic site of CHE hydrogenation were also different from those obtained from the HDS reaction of thiophene (623 K and 7.0 MPa) (6).

In accordance with a previous investigation of the hydrogenation of CHE in the presence of piperidine (16), it was found that in the presence of OPA and NH_3, the effective rate constants ($k_{CHE}K_{CHE}/(1+K'_iP_i)$) of the hydrogenation reaction were lower over the NiMoP/Al_2O_3 catalyst, demonstrating that phosphorus has a negative effect on the hydrogenation of CHE. In the absence of these

TABLE 6

The Effective Rate Constants and Adsorption Constants in the Hydrogenation of CHE at 593–643 K, 3.0 MPa, and $P_{H_2S} = 6.5$ kPa

Catalyst	Temp. (K)	$k_{CHE}K_{CHE}/(1+K'_iP_i)$ (s^{-1})			Adsorption constant (kPa^{-1})	
		CHE alone	CHE + OPA	CHE + NH_3	K'_{OPA}	K'_{NH_3}
NiMo/Al_2O_3	593	16	3.8	6.8	0.67	1.0
NiMoP/Al_2O_3	593	22	2.6	5.7	1.6	1.7
NiMo/Al_2O_3	623	25	9.0	13	0.41	0.54
NiMoP/Al_2O_3	623	34	6.5	14	0.89	0.96
NiMo/Al_2O_3	643	32	12	20	0.35	0.4
NiMoP/Al_2O_3	643	43	9.3	19	0.76	0.76

Note. $P^0_{OPA} = 4.8$ kPa, $P^0_{NH_3} = 1.6$ kPa.

TABLE 7

A Comparison of the Effective Rate Constant of the Hydrogenation of EB and CHE at 593 K and 3.0 MPa [s^{-1}]

Catalyst	$P_{H_2S} = 6.5$ kPa		$P_{H_2S} = 0$	
	$k_{CHE}K_{CHE}$	$k_{EB}K_{EB}$	$k_{CHE}K_{CHE}$	$k_{EB}K_{EB}$
$NiMo/Al_2O_3$	16	0.044	69	0.18
$NiMoP/Al_2O_3$	22	0.063	98	0.35

nitrogen-containing compounds, however, phosphorus has a promotive effect on the effective rate constants (Table 6). This shows that the negative effect of phosphorus on the hydrogenation of an olefin in the presence of nitrogen-containing compounds is not due to the intrinsic kinetics, but to the stronger inhibition by adsorption of the nitrogen-containing compounds over the $NiMoP/Al_2O_3$ catalyst relative to the $NiMo/Al_2O_3$ catalyst. Although the HDN of OPA and hydrogenation of CHE take place on different catalytic sites, OPA adsorbs on the catalytic site for the hydrogenation of CHE as well and hinders this hydrogenation reaction.

Although phosphorus has a negative effect on the hydrogenation of EB in the simultaneous reactions of EB and OPA (Table 2), a separate hydrogenation study of pure EB shows that the hydrogenation of aromatics was also enhanced by the presence of phosphorus in the catalyst (Table 7). However, the hydrogenation reactivity of EB is strongly different from that of aniline, as shown by the much smaller rate constant of EB compared to that of OPA, which may be due to their adsorption orientations over the catalysts or different hydrogenation mechanisms. The effects of phosphorus and inhibition on the hydrogenation of EB are similar to those in the hydrogenation of CHE; they indicate again that the stronger inhibition effect of the nitrogen-containing compounds over the $NiMoP/Al_2O_3$ catalyst accounts for the overall negative effect of phosphorus in the simultaneous hydrogenation reaction of phenyl as well as olefin groups.

3.3. Fitting of the HDN network. The complete HDN network (Fig. 1b) could be uniquely fitted once the adsorption constants of OPA in the HDN and hydrogenation reactions, the HDN rate constants k_1 and k_2, and the adsorption constants of OPA and NH_3 on the hydrogenation site were known. Although the best fit was obtained when assuming that there was a direct reaction route from OPA to PCH, the rate constant of this reaction path was much smaller than k_2 and k_4, and the fitting confidence range of this rate constant was much wider. Therefore, the direct conversion of OPA to PCH (via PCHA) was neglected in the network fitting. Further work should demonstrate how much slower the direct hydrogenolysis of propylcyclohexylamine really is relative to the elimination reaction.

Assuming that the HDN of OPA and hydrogenation of CHE take place on two different catalytic sites and follow the Langmuir–Hinshelwood mechanism, we have

$$-\frac{dP_{OPA}}{d\tau} = \frac{(k_1 + k_2)K_{OPA}P_{OPA}}{1 + K_{OPA}P_{OPA} + K_{NH_3}P_{NH_3}} \quad [8.1]$$

$$\frac{dP_{PCHE}}{d\tau} = \frac{k_2 K_{OPA}P_{OPA}}{1 + K_{OPA}P_{OPA} + K_{NH_3}P_{NH_3}} - \frac{(k_3 + k_4)K_{PCHE}P_{PCHE}}{1 + K'_{OPA}P_{OPA} + K'_{NH_3}P_{NH_3}} \quad [8.2]$$

$$\frac{dP_{PB}}{d\tau} = \frac{k_1 K_{OPA}P_{OPA}}{1 + K_{OPA}P_{OPA} + K_{NH_3}P_{NH_3}} + \frac{k_3 K_{PCHE}P_{PCHE}}{1 + K'_{OPA}P_{OPA} + K'_{NH_3}P_{NH_3}} \quad [8.3]$$

$$\frac{dP_{PCH}}{d\tau} = \frac{k_4 K_{PCHE}P_{PCHE}}{1 + K'_{OPA}P_{OPA} + K'_{NH_3}P_{NH_3}} \quad [8.4]$$

$$P_{NH_3} = P^0_{OPA} - P_{OPA}, \quad [8.5]$$

where K'_{OPA} and K'_{NH_3} are the adsorption constants of OPA and NH_3 on the catalytic site for olefin hydrogenation (the same as for CHE) respectively; k_3 is the rate constant for the dehydrogenation of PCHE to PB; and k_4 and K_{PCHE} are the rate and adsorption constants of hydrogenation of PCHE to PCH, respectively.

The confidence range of the fitted parameters was improved if the hydrogenation network of CHE was fitted together with the HDN network of OPA with the simultaneous reaction of OPA + CHE, especially the confidence range of k_4K_{PCHE}. An example of this two-site model fitting is given in Fig. 8, and the resulting kinetic parameters

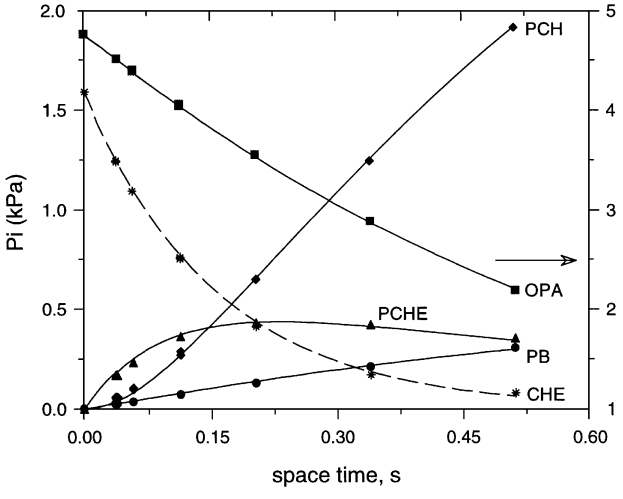

FIG. 8. Simultaneous regression of the HDN network of OPA and hydrogenation of CHE over $NiMoP/Al_2O_3$ at 623 K and 3.0 MPa (points, experimental data; lines, prediction).

TABLE 8

Rate and Adsorption Constants and Their Confidence Ranges in the HDN Network of OPA at 593–643 K, 3.0 MPa, and P_{H_2S} = 6.5 kPa (k in [kPa · s^{-1}] and K in [kPa^{-1}])

Constant	Temp. (K)	NiMo/Al_2O_3 Value	NiMo/Al_2O_3 Low[a]	NiMo/Al_2O_3 High[a]	NiMoP/Al_2O_3 Value	NiMoP/Al_2O_3 Low[a]	NiMoP/Al_2O_3 High[a]
k_3K_{PCHE}	593	0			0		
k_4K_{PCHE}		27	26	28	40	38	42
K_{NH_3}		2.3	2.0	2.5	2.9	2.3	3.4
k_3K_{PCHE}	623	1.0	0.6	1.4	0.9	0.4	1.4
$k4_5K_{PCHE}$		42	40	45	55	53	56
K_{NH_3}		0.53	0.49	0.57	1.0	0.9	1.0
k_3K_{PCHE}	643	2.7	2.4	3.1	3.3	2.4	4.0
k_4K_{PCHE}		54	52	56	75	69	81
K_{NH_3}		0.31	0.30	0.32	0.34	0.32	0.37

[a] 95% confidence range.

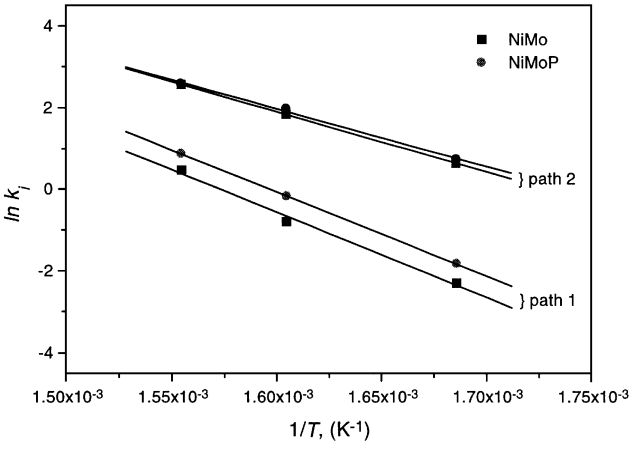

FIG. 9. Arrhenius plot of the HDN rate constant of OPA over NiMo(P)/Al_2O_3.

are given in Table 8. The 95% confidence ranges of these fitted parameters are usually within ±20% variance of the parameter values, demonstrating the effectiveness of the fitting to the experimental data and the present modeling method.

It is found from Table 8 that the dehydrogenation of PCHE to PB can be neglected at low reaction temperatures. The ratios k_3/k_4 (around 0.02 at 623 K and 0.04 at 643 K) and k_1/k_2 (around 0.1 at 623 K and 0.14 at 643 K) indicate that PB in the HDN product comes largely from the direct C(sp^2)–N bond cleavage of OPA. This demonstrates that one can judge the relative contributions of the HDN reaction through the OPA → HC path and the DHQ → PCHA → HC path in the HDN network of quinoline-type compounds by evaluating the concentration of PB in the HDN products (18, 19), since the HDN reaction through the latter reaction path hardly results in PB.

A comparison of Tables 7 and 8 shows that the effective rate constants of the hydrogenation of PCHE ($k_{PCHE}K_{PCHE}$) in the HDN network of OPA and the effective rate constant of the hydrogenation of CHE ($k_{CHE}K_{CHE}$) show the same trend with the catalysts and reaction temperatures, confirming the validity of our kinetic approach and indicating that the hydrogenation of PCHE and CHE takes place on the same catalytic site. The somewhat higher effective rate constant of the hydrogenation of PCHE might be due to a larger adsorption constant, because of its molecular structure.

DISCUSSION

The activation energies of the HDN reaction paths 1 and 2 were calculated according to the Arrhenius equation (Fig. 9). They show no significant difference between the NiMo/Al_2O_3 and NiMoP/Al_2O_3 catalysts (Table 9), suggesting that mainly the number of the catalytic sites has increased by the introduction of phosphorus while the intrinsic activity of the sites has remained unchanged.

The activation energy of reaction path 1 is higher than that of reaction path 2 (Table 9), in agreement with the observation of Shabtai *et al.*, who reported a higher activation energy for the direct C(sp^2)–N bond cleavage (206 kJ/mol) than for the aromatics hydrogenation (165 kJ/mol) in the HDN of 5,6-benzoquinoline (34). The higher activation energy of reaction path 1 means that direct C(sp^2)–N bond cleavage of OPA is favored at higher reaction temperatures. This explains why lower PCH/PB ratios were observed in the HDN product at higher reaction temperatures, since direct C(sp^2)–N bond cleavage reaction results in the formation of PB which usually cannot be converted further under HDN conditions (Table 2). This is also the case for the HDN of quinoline, where the HDN reaction through the intermediate OPA is an important source of PB formation (19).

Just like the activation energies, the heats of adsorption of OPA on the catalytic sites for HDN and hydrogenation show no difference between the P-containing and P-free catalysts either (Fig. 10, Table 10). The larger value of the adsorption constant $K_{ads} = \exp(-\Delta H_{ads}/RT) \cdot \exp(\Delta S_{ads}/R)$ for the P-containing catalyst must be ascribed to an entropy effect, meaning that the adsorbed OPA molecule loses less

TABLE 9

Temperature Dependence of the Reaction Rate Constants $k = k_0 \cdot \exp(-E/RT)$ in the HDN of OPA at 3.0 MPa (P_{H_2S} = 6.5 kPa)

Arrhenius constants	NiMo/Al_2O_3 Path 1	NiMo/Al_2O_3 Path 2	NiMoP/Al_2O_3 Path 1	NiMoP/Al_2O_3 Path 2
E (kJ/mol)	174	122	171	117
k_0 (kPa/s)	1.9×10^{14}	11×10^{10}	2.0×10^{14}	4.8×10^{10}

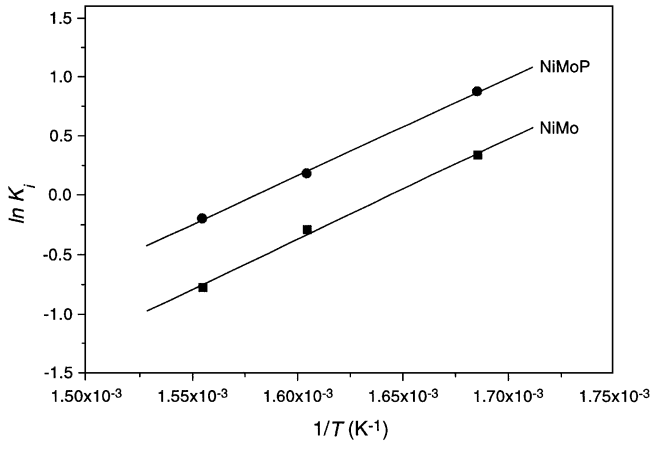

FIG. 10. Temperature dependence of the adsorption constants of OPA over NiMo(P)/Al_2O_3.

entropy. This may be due to geometrical constraints. In combination with the activation energies, these results indicate that phosphorus increases the number of catalytic sites in the sulfided NiMo(P)Al_2O_3 catalysts for the HDN of OPA, but does not change the nature of the sites. Therefore, phosphorus does not participate directly in the HDN reaction, and neither are the reactant/intermediates directly activated over phosphorus.

It is accepted that the edges and corners of the MoS_2 crystallites on the catalyst carry the active sites for the hydrotreating reactions (35–37). Especially for the hydrogenation reaction, surface coordinatively unsaturated Mo atoms at the edges or corners are believed to be these active sites (32, 38). Since HDN of OPA takes place mainly through reaction path 2 which is limited by the hydrogenation of the phenyl group, the present results may be interpreted as indicating that the modification of the catalytic sites for HDN path 2 by phosphorus over the NiMo/Al_2O_3 catalyst is due to increased stacking of MoS_2 slabs (39, 40). This increased stacking may lead to different amounts of rim, edge, and basal sites (41), and account for the increased number of accessible catalystic sites. Also the difference in adsorption entropy can be explained with stacking: a reactant molecule will have more rotational freedom when it is adsorbed at the edge of a MoS_2 sandwich layer at the top of a stack of MoS_2 layers, than at a single MoS_2 layer flat on the MoS_2 support. As a consequence, the molecule loses less degrees of freedom upon adsorption and the loss of entropy will be smaller.

Our results do not rule out that some surface S^{2-} ions are replaced by P^{3-} anions (13, 42), with the consequence that some Mo(Ni) sites become more electron-rich because of the less electron-negative properties of phosphorus than of sulfur. This may lead to an increased number of catalytic sites for HDN path 1, as the direct C(sp^2)–N bond cleavage has been shown to take place on a catalytic site with more electron-donating features (12). This would be consistent with the observation that over metallic Mo_2N catalysts (43) direct C(sp^2)–N bond cleavage is strongly favored. However, it should be kept in mind that direct C(sp^2)–N bond cleavage of OPA occurs to a limited extent over sulfided NiMo(P)/Al_2O_3 catalysts only.

The heats of adsorption of OPA and NH_3 were higher over the HDN catalytic site than over the olefin hydrogenation site (Table 10). This further demonstrates that different kinds of catalytic sites on the sulfided catalyst are responsible for the hydrogenation of an olefin group and of the phenyl group in an aniline molecule, and that by modifying the ratio of these sites, it should in principle be possible to modify the selectivity of a catalyst toward different reactions.

The present study shows that one can learn a lot about the nature of the catalytic sites and the function of the catalytic components when a careful kinetic study is performed. It also shows how complicated a kinetic study for a relatively simple HDN network like that of OPA already is. This complication arises from mainly the strong adsorption of the nitrogen-containing reactants, intermediates, and products over a variety of catalytic sites involved in the different reaction steps. Different sites and adsorption constants must be used to quantify their effects. A variation of the initial reactant partial pressure and performing simultaneous reactions are efficient ways of determining the adsorption constants and unraveling the kinetic network.

TABLE 10

Temperature Dependence of the OPA Adsorption Constants $K = K_0 \cdot \exp(-\Delta H_{ads}/RT)$ on the HDN Site and Hydrogenation (HG) Site at 3.0 MPa ($P_{H_2S} = 6.5$ kPa)

	NiMo/Al_2O_3		NiMoP/Al_2O_3	
Arrhenius constants	HDN site	HG site	HDN site	HG site
$-\Delta H_{ads}$ (kJ/mol)	70	42	68	44
K_0 (kPa^{-1})	9.9×10^{-7}	1.3×10^{-4}	23×10^{-7}	1.9×10^{-4}

CONCLUSIONS

The observation of PCHA showed that hydrogenation of the phenyl ring is one of the first reaction steps in the HDN of OPA, and that the presence of the amine substituent strongly facilitated this hydrogenation. Phosphorus exhibited a promotive effect on the HDN of OPA, which arises from the more favorable adsorption of OPA on the phosphorus-containing catalyst as well as from the increased number of catalytic sites. The increased number of catalytic sites for the hydrogenation of the phenyl ring (HDN path 2) was interpreted by a geometrical effect, due to the increased stacking of MoS_2 layers. The increased

adsorption constant was ascribed to more rotational freedom of OPA after adsorption, and thus to a smaller loss in adsorption entropy.

The adsorption constant for OPA in the HDN reaction proved to be different from that in the hydrogenation of CHE. This indicates that the hydrogenation of the phenyl group in an aniline molecule and the hydrogenation of an alkene take place over different catalytic sites. The presence of phosphorus in a $NiMo/Al_2O_3$ catalyst shows a promotive effect on both hydrogenation reactions. The fact that nevertheless an overall negative effect of phosphorus on the alkene hydrogenation in the presence of nitrogen-containing compounds was observed is not due to the intrinsic kinetics, but due to the stronger adsorption of the nitrogen-containing compounds on the catalyst thus inhibiting the hydrogenation reaction.

A Langmuir–Hinshelwood model with different sites for HDN and hydrogenation has been effectively applied in the kinetic study of the HDN network of OPA. The direct modeling of the kinetic HDN results proved impossible, because no mathematically unique solution could be found. It was necessary to first determine a few parameters in an independent manner before a unique regression of the experimental data could be performed. Calculation of the kinetic parameters could be efficiently done through variation of the initial reactant partial pressure and through simultaneous reactions.

REFERENCES

1. Schulz, H., Schon, M., and Rahman, N. M., *Stud. Surf. Sci. Catal.* **27**, 201 (1986).
2. Ho, T. C., *Catal. Rev. Sci. Eng.* **30**, 117 (1988).
3. Girgis, M. J., and Gates, B. C., *Ind. Eng. Chem. Res.* **30**, 2021 (1991).
4. Perot, G., *Catal. Today* **10**, 447 (1991).
5. Nagai, M., Sato, T., and Aiba, A., *J. Catal.* **97**, 52 (1986).
6. La Vopa, V., and Satterfield, C. N., *J. Catal.* **110**, 375 (1988).
7. Vivier, L., and Perot, G., *in* "Proceedings, 12th Ibero-American Symposium on Catalysis, Rio de Janeiro," Vol. 2, p. 582 (1990).
8. Ho, T. C., Katritzky, A. R., and Cato, S. J., *Ind. Eng. Chem. Res.* **31**, 1589 (1992).
9. Kasztelan, S., des Courières, T., and Breysse, M., *Catal. Today* **10**, 433 (1991).
10. Geneste, P., Moulinas, C., and Olivé, J. L., *J. Catal.* **105**, 254 (1987).
11. Perot, G., Brunet, C., Canaff, C., and Toulhoat, H., *Bull. Soc. Chim. Belg.* **96**, 865 (1987).
12. Moreau, C., Joffre, J., Saenz, C., and Geneste, P., *J. Catal.* **122**, 448 (1990).
13. Jian, M., and Prins, R., *Catal. Today* **30**, 127 (1996).
14. Callant, M., Holder, K. A., Grange, P., and Delmon, B., *Stud. Surf. Sci. Catal.* **100**, 199 (1996).
15. Jian, M., and Prins, R., *Catal. Lett.* **35**, 193 (1995).
16. Jian, M., Rico Cerda, J. L., and Prins, R., *Bull. Soc. Chem. Belg.* **103**, 225 (1995).
17. Satterfield, C. N., and Yang, S. H., *Ind. Eng. Chem. Process Des. Dev.* **23**, 11 (1984).
18. Jian, M., and Prins, R., *Stud. Surf. Sci. Catal.* **101**, 87 (1996).
19. Jian, M., and Prins, R., to be published.
20. Satterfield, C. N., and Gültekin, S., *Ind. Eng. Chem. Process Des. Dev.* **20**, 62 (1981).
21. Cerny, M., *Coll. Czech. Chem. Commun.* **47**, 928 (1982).
22. Yang, S. H., and Satterfield, C. N., *J. Catal.* **81**, 168 (1983).
23. Yang, S. H., and Satterfield, C. N., *Ind. Eng. Chem. Process Des. Dev.* **23**, 20 (1984).
24. Perot, G., Brunet, S., and Hamze, N., *in* "Proceedings, 9th Int. Congress Catal.," Vol. 1, p. 19 (1988).
25. Laurent, E., and Delmon, B., *Ind. Eng. Chem. Res.* **32**, 2516 (1993).
26. Callant, M., Holder, K. A., Grange, P., and Delmon, B., *Bull. Soc. Chim. Belg.* **104**, 245 (1995).
27. Stuchly, V., and Beranek, L., *Appl. Catal.* **35**, 35 (1987).
28. Gevert, B. S., Otterstedt, J.-E., and Massoth, F. E., *Appl. Catal.* **31**, 119 (1987).
29. Moreau, C., Aubert, C., Durand, R., Zmimita, N., and Geneste, P., *Catal. Today* **4**, 117 (1988).
30. Okamoto, Y., Maezawa, A., and Imanaka, A., *J. Catal.* **120**, 29 (1989).
31. Massoth, F. E., Balusami, K., and Shabtai, J., *J. Catal.* **122**, 256 (1990).
32. Delmon, B., *Bull. Soc. Chim. Belg.* **104**, 173 (1995).
33. Jian, M., and Prins, R., *Bull. Soc. Chem. Belg.* **103**, 231 (1995).
34. Shabtai, J., Yeh, G. J. C., Russell, C., and Oblad, A. G., *Ind. Eng. Chem. Res.* **28**, 139 (1989).
35. Topsøe, H., Clausen, B. S., Topsøe, N.-Y., and Pedersen, E., *Ind. Eng. Chem. Fundam.* **25**, 25 (1986).
36. Knözinger, H., *in* "Proceedings, 9th Int. Congress Catal." (M. J. Phillips and M. Ternan, Eds.), Vol. 5, p. 20. The Chemical Institute of Canada, 1988.
37. Prins, R., de Beer, V. H. J., and Somorjai, G. A., *Catal. Rev. Sci. Eng.* **31**, 1 (1989).
38. Kasztelan, S., Jalowiecki, J., Wambeke, A., Grimblot, J., and Bonnelle, J. P., *Bull. Soc. Chim. Belg.* **96**, 1003 (1987).
39. Ryan, R. C., Kemp, R. A., Smegal, J. A., Denley, D. R., and Spinnler, G. E., *Stud. Surf. Sci. Catal.* **50**, 21 (1989).
40. Payen, E., Hubaut, R., Kasztelan, S., Poulet, O., and Grimblot, J., *J. Catal.* **147**, 123 (1994).
41. Daage, D., and Chianelli, R., *J. Catal.* **149**, 414 (1994).
42. Mangnus, P. J., van Langeveld, A. D., de Beer, V. H. J., and Moulijn, J. A., *Appl. Catal.* **68**, 161 (1991).
43. Lee, K. S., Abe, H., Reimer, J. A., and Bell, A. T., *J. Catal.* **139**, 34 (1993).